Modeling Migration, Compartmentalization and Exit of Naive T Cells in Lymph Nodes Without Chemotaxis

Johannes Textor[1] and Jürgen Westermann[2]

[1] Institut für Theoretische Informatik
[2] Institut für Anatomie
Universität zu Lübeck, 23538 Lübeck, Germany

textor@tcs.uni-luebeck.de

Abstract. The migration of lymphocytes through secondary lymphoid organs was believed to be mainly controlled by chemokine gradients. This theory has recently been called into question since naive lymphocytes observed *in vivo* by two-photon microscopy show no evidence of directed migration. We have constructed a simple mathematical model of naive T cell migration in lymph nodes that is solely based on local mechanisms. The model was validated against findings from histological analysis and experimentally determined lymphocyte recirculation kinetics. Our results suggest that T cell compartmentalization in lymph nodes can be explained without long-range chemokine gradients. However, the T cell residence time predicted by our model is significantly lower than observed *in vivo*, indicating the existence of a mechanism which alters the T cell random walk over time.

1 Introduction

Immune responses are mounted and supervised in secondary lymphoid organs (SLOs). These functions are crucial: loss of all secondary lymphoid organs leads to death. Among the several kinds of SLOs, i.e. lymph nodes, Peyer's patches and the spleen, the mass of lymph nodes makes up about 60% [1].

Unlike many other organs which consist mainly of *resting* cells, SLOs mostly contain highly *motile* cells: Lymphocytes perpetually enter, move within, and exit from SLOs. This restlessness is important because a previously unseen antigen is sometimes only recognizable by a few dozen out of several millions of lymphocytes. Since infections are usually local, the right cell being at the wrong place may mean that the immune response is mounted too late. Additionally, many essential functions of lymphocytes are *contextual*, i.e. restricted to a certain environment. For instance, somatic hypermutation of B cells is mainly restricted to germinal centers. Thus, in order to understand lymphocyte *function*, it is essential to study their *migration* [2].

On their endless journey, lymphocytes are often guided by chemotaxis [3–5]. For example, chemokines control the recruitment of circulating lymphocytes

into SLOs. Knowledge of these mechanisms has important clinical implications: chemokine receptors controlling lymphocyte migration have repeatedly proved to be excellent targets for the inhibition of inflammatory diseases like atopic dermatitis or multiple sclerosis [6]. Unsurprisingly, it has been proposed that chemokines also control the migration of lymphocytes *within* lymph nodes and other SLOs (e.g. [4]).

However, this theory has recently been called into question [7]: By two-photon microscopy, it has become possible to observe individual cells in the intact lymph node *in vivo* [8, 9]. It was found that naive T cells show no sign of directed migration, as they would under the influence of chemokine gradients. Rather, their motion is best described as a random walk [7, 10–13].

Our goal is a better understanding of these new results. In particular, we are interested in three aspects: (i) *migration* of naive T cells within lymph nodes; (ii) *compartmentalization* (see Fig. 1) of the constantly moving cells and; (iii) *exit* of naive T cells from the lymph node. We know that the entry of lymphocytes into SLOs is controlled by chemokine gradients – does the same apply to migration, compartmentalization and exit?

To address these questions, we have constructed a simple mathematical model that does not use chemotaxis, but is solely based on local mechanisms. Compartmentalization is explained by assuming that naive T cells *prefer* to walk along the fibers of the FDC network which makes up the paracortex, but *retain* their normal motility when outside of this network. Entry and exit are modelled as uniformly distributed processes in the paracortex and the medulla, respectively. We have found that these minimal assumptions give rise to dynamics that reasonably match recirculation dynamics and compartmentalization observed *in vivo*. Our results suggest that chemotaxis is not necessary to explain the forming of the lymph node compartments. However, the T cell residence time predicted by our model is significantly lower than in reality. This may indicate the existence of a mechanism which alters the motility of naive T cells over time, as it was shown to be the case for T cells which are stimulated by antigen [13].

2 Background

The basic structure of a lymph node is shown in Fig. 2. Both B and T cells enter through the *high endothelial venules* in the paracortical area. These capillary vessels bear molecules which "recruit" circulating lymphocytes from the blood stream. Presentation of processed antigen to T cells by dendritic cells takes place in the *paracortex*. In this densely packed environment, T cells and dendritic cells have frequent, short-lasting contacts. B cells, on the other hand, migrate to the *cortex* where they screen *follicular dendritic cells* for native antigen. The existence of designated lymph node compartments for B and T cells thus makes the search for antigen of both subpopulations more efficient. Upon activation, both B and T cells migrate towards the border between cortex and paracortex. Here, they exchange the costimulatory signals that initiate germinal center formation and with it the Th2 immune response [14]. This is why the existence of a real

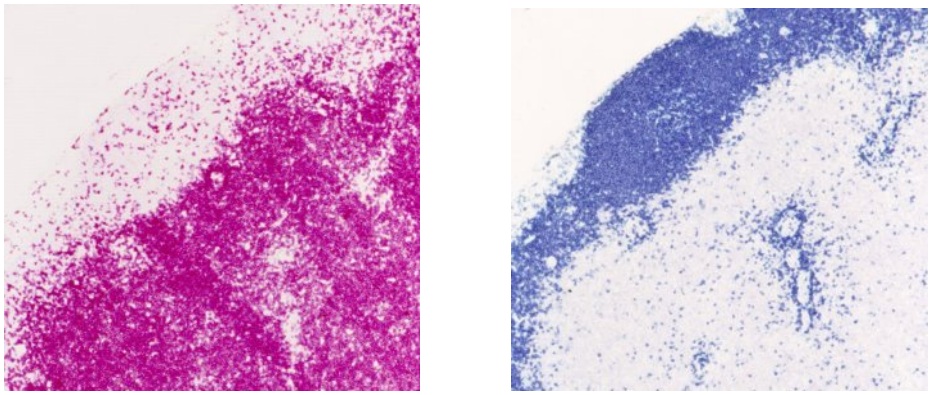

Fig. 1. Cortex and paracortex in slices of an uninfected lymph node of a rat (source: own work) with colored T cells (left) and colored B cells (right). High endothelial venules appear as "holes" in the paracortex.

physical barrier between the two compartments is neither likely nor desirable: upon antigen challenge, it would stand in the way of germinal center formation.

Due to the absence of a physical barrier, it was long unclear how the separation between T and B cell areas in lymph nodes is established and maintained. Visually, the two areas are not distinguishable. Most likely, paracortex and cortex are defined by different types of stromal cells. In the paracortex, the *fibroblastic reticular cells* (FRCs) dominate. The best defined stromal cell subset in the cortex are the follicular dendritic cells (FDCs) that present native antigen to B cells [5, 15]. Bajénoff et al. [10] have recently demonstrated *in vivo* that T cells move along the fibers of the FRC network while B cells walk along the FDC network.

Still, these findings do not completely rule out the possibility that chemokines play a role in defining cortex and paracortex. First of all, the mentioned migration of activated T and B cells towards the cortex/paracortex boundary is controlled by chemokines made by the FRCs and FDCs [4]. These gradients might also affect naive lymphocytes. Due to technical issues, two-photon imaging experiments are limited to a timeframe of about 1-2 hours [8]. This is short compared to the 24 hours lymphocytes typically spend in lymph nodes. Weak chemokine gradients that only create a small bias in lymphocyte motility might not be detected by this method. Such gradients might have an important effect on the long-term dynamics, especially on the exit process. Formal modeling is helpful to shed light on these contradicting theories.

Our starting point was a simple hypothesis on how cortex and paracortex are formed: It makes no difference if T cells are released in the cortex or in the paracortex. They retain their normal motility pattern (this has been confirmed by Miller et al. [11]) and, when inside the cortex, do not use chemotaxis to find back to the paracortex. When approaching the cortex from the paracortex, the FRC network becomes more sparse. Under these circumstances, T cells will

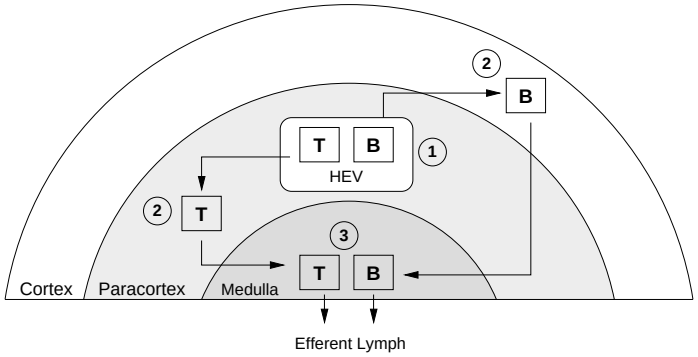

Fig. 2. Schematic representation of lymphocyte migration through the lymph node: (1) Lymphocytes enter the lymph node through high endothelial venules in the paracortex. (2) T cells remain in this compartment, while B cells migrate to the cortex. (3) B and T cells exit the lymph node via efferent lymphatic vessels which drain the medulla.

preferentially, but not exclusively, move along the remaining FRC fibers. This simple effect should already give rise to compartmentalization.

This gave rise to the idea of constructing a simple model which does not include chemotaxis, but is only based on local mechanism as the one described above, and validate it against experimental results from histological analysis and recirculation experiments. We hoped that this model would give us a better understanding of the nature of the boundary and compartments generated by the defined mechanism. Moreover, it would show whether the kinetics of lymphocyte recirculation could really be the result of a simple uniform random walk.

3 The Model

Several authors (e.g. [16, 17]) proposed agent-based models of cellular interactions in the lymph node. These models are very useful to study the complex emergent aspects of the immune response like affinity maturation. However, they are too complex for our purpose, since we are focusing on naive cells. Beltman et al. [18, 19] studied the dynamics of naive T cell migration using a cellular Potts model which focuses on the paracortex. This model is impressively consistent with experimental results from two-photon microscopy. Yet, we found it too complicated to incorporate medulla and paracortex into this model and decided to start with a simpler approach. Stekel et al. [20, 21] studied the dynamics of lymphocyte recirculation using differential equations, but they did not model the lymph node compartments explicitly.

Compared to these approaches, our model is situated on an intermediate (mesoscopic) scale. We abstract from the individual cells and use scale-free concentrations instead, but represent the lymph node compartments explicitly. We have deduced the sizes and shapes of the compartments from the literature (see

table 1) and from our own experiments and archived microtome slices. However, it must be taken into account that lymph node morphology varies considerably. For example, many lymph nodes show a concave boundary from medulla to paracortex (see e.g. [15]) instead of the convex one used in our model.

We focus on T cells since the available data on their motility patterns is much more detailed and reliable than that of B cells. This is partially due to technical difficulties with unambiguously monitoring B cells in the paracortex [10]. We plan to gradually incorporate B cells into our model as more reliable experimental results become available.

Our model is based on a three-dimensional grid. The edges of this grid represent the network of FRC and FDC processes in the lymph node. As shown in Fig. 3, the grid is subdivided into three zones, which represent the cortex, the paracortex and the medulla. The T cells are not represented individually, but as abstract, scale-free concentrations, which allows for larger-scale simulations, but sacrifices stochasticity. Our assumption that T cells migrate only by uniform random motion, except on the border from paracortex to cortex where they are more likely to remain in the paracortex, then corresponds to a diffusion process of the T cell concentration.

In the next two sections, we give a detailed formal definition of the model. It is primarily aimed at those who wish to reproduce our results and is thus written in a rather condensed form. Readers who are unfamiliar with lattice diffusion models should consult additional literature. For example, a similar two-dimensional model has been used to simulate the spread of Influenza infections on a cell monolayer [22]. A general introduction to models of diffusion which also covers reaction-diffusion and chemotaxis is given in Murray [23], Chap. 11.

3.1 Basic Structure and Evolution Equations

Let $\mathcal{LN} \subset R^3$ be a simply-connected smoothly bounded region (e.g. an ellipsoid) that is subdivided into three pairwise disjoint regions $\mathcal{M}, \mathcal{P}, \mathcal{C}$. We discretize $\mathcal{LN}$ by an isotropic cubic lattice $L = (V, E)$ with vertices $V = \{(n_x \Delta s, n_y \Delta s, n_z \Delta s) : n_x, n_y, n_z \in \mathbb{Z}\}$ and edges $E = \{(v, v') \in V \times V : ||v - v'|| = 1\}$. The set of neighbours of $v \in \mathcal{LN}$ is written as $v^+(v) = \{w \in V : (v, w) \in E \wedge w \in \mathcal{LN}\}$. We additionally define $c^+(v) = v^+(v) \cap \mathcal{C}$. The interval $\{x \in \mathbb{R} : 0 \leq x \leq 1\}$ is denoted by $[0, 1]$.

An edge coloring $f(v, w) : E \mapsto \{0, 1\}$ represents the network of stromal follicular dendritic cells in the paracortex and fibroblastic reticular cells in the cortex: $f(v, w) = 1 \Leftrightarrow v \in \mathcal{C} \vee w \in \mathcal{C}$. The boundary between the compartments is denoted by $\mathcal{B} = \{v \in \mathcal{P} : c^+(v) \neq \emptyset\}$.

The distribution of T cells across the lymph node at time t is given by the function $T : \mathbb{R} \times \mathbb{V} \mapsto \mathbb{R}_0^+$. Our model evolves in discrete time steps $n\Delta t, n \in \mathbb{N}$. Entry, random walk, and exit of T cells are modeled by evolution equations, analogous to finite difference approximations of differential equations.

Three kinetic parameters apply during each time step t: $\boldsymbol{e}(t, v) \in \mathbb{R}_0^+$ denotes the unitless amount of new T cells that enter a vertex $v \in \mathcal{P}$ from HEVs, which are not modeled explicitly. From every $v \in V$, a fraction $\boldsymbol{m} \in [0, 1]$ out of $T(t, v)$

moves to one of the neighbouring vertices. For $v \in \mathcal{M}$, a fraction $\boldsymbol{l} \in [0,1]$ of $(1-\boldsymbol{m})T(t,v)$ exits (leaves) from v. The structural parameter $\boldsymbol{\sigma} \in [0,1]$ is a measure of the "stickiness" of T cells to FRC fibers. Altogether, the evolution equation of $T(t,v)$ for $v \in \mathcal{P}$ is defined as follows:

$$\begin{aligned} T(t+\Delta t,v) = \boldsymbol{e}(t,v) + (1-\boldsymbol{m})\,T(t,v) + \sum_{w \in v^+(v)\setminus\mathcal{B}} \frac{\boldsymbol{m}}{|v^+(w)|} T(t,w) \\ + \sum_{w \in v^+(v)\cap\mathcal{B}} \frac{|v^+(w)| - (1-\boldsymbol{\sigma})|c^+(w)|}{|v^+(w)\setminus c^+(w)|} \frac{\boldsymbol{m}}{|v^+(w)|} T(t,w) \end{aligned} \tag{1}$$

On $v \in \mathcal{M}$, we use:

$$\begin{aligned} T(t+\Delta t,v) = \boldsymbol{l}\,(1-\boldsymbol{m})\,T(t,v) + \sum_{w \in v^+(v)\setminus\mathcal{B}} \frac{\boldsymbol{m}}{|v^+(w)|} T(t,w) \\ + \sum_{w \in v^+(v)\cap\mathcal{B}} \frac{|v^+(w)| - (1-\boldsymbol{\sigma})|c^+(w)|}{|v^+(w)\setminus c^+(w)|} \frac{\boldsymbol{m}}{|v^+(w)|} T(t,w) \end{aligned} \tag{2}$$

And for $v \in \mathcal{C}$, we obtain:

$$\begin{aligned} T(t+\Delta t,v) = (1-\boldsymbol{m})\,T(t,v) + \sum_{w \in v^+(v)\setminus\mathcal{B}} \frac{\boldsymbol{m}}{|v^+(w)|} T(t,w) \\ + \sum_{w \in v^+(v)\cap\mathcal{B}} (1-\boldsymbol{\sigma}) \frac{\boldsymbol{m}}{|v^+(w)|} T(t,w) \end{aligned} \tag{3}$$

Setting $\boldsymbol{e}(t,v) = \boldsymbol{l} = 0$ for all v and t, (1) to (3) reduce compartment-wise to a discrete version of the continuous diffusion equation

$$\frac{\partial T}{\partial t} = D\nabla^2 T \qquad \text{where } D\frac{\Delta s^2}{\Delta t} = \boldsymbol{m}$$

which describes a discrete random walk. On the boundary of $\mathcal{LN}$, the random walk is "myopic": Since the fraction of T that is transferred to the neighbouring nodes is always $\boldsymbol{m}$, a higher relative amount is transferred along each adjacent edge. Thus, in equilibrium, boundary vertices v' hold a fraction of $v^+(v')/6$ of the concentration of non-boundary cells. This must be taken into account when calculating region-wise mean concentrations.

From numerical analysis, it is known that a finite difference approximation of the diffusion equation where $D\Delta t/\Delta s^2 > 0.5$ is unstable. In our model, $\boldsymbol{m} > 0.5$ could lead to a periodic random walk ("chessboard pattern") and thus to meaningless results. Thus, for explicit simulations, Δt must be sufficiently small.

The lattice spacing Δs may be set to the mean stromal cell network spacing of $20\mu m$ [10], but other sufficiently small values are also valid as long as $\boldsymbol{m}$ is scaled to reproduce the motility coefficient of T cells of about $67\mu m^2/\text{min}$ [11, 12]. Reasonable values for $\boldsymbol{l}$ and $\boldsymbol{\sigma}$ will be derived in Sec. 4.

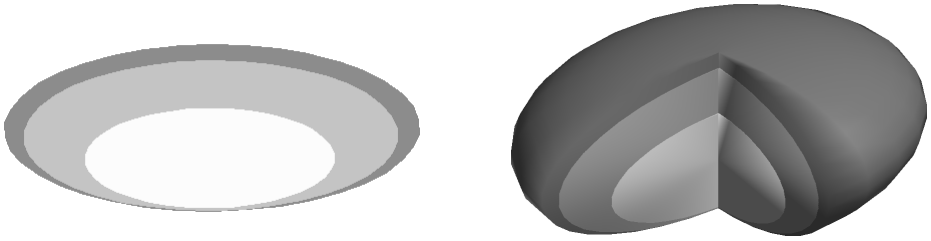

Fig. 3. Structure of our lymph node model. Medulla (innermost region), paracortex and cortex (outermost region) are delimited by ellipsoids as defined in Sec. 3.2. Left: 2D planar section. Right: 3D structure. Parameters are given in table 1.

3.2 Lattice Topology

Size, shape and structure of $\mathcal{LN}$ are characterized by the 6 parameters $r_{\mathcal{M}} < r_{\mathcal{P}} < r_{\mathcal{C}} \in \mathbb{R}_0^+, a_x, a_y, a_z \in [0,1]$. $\mathcal{M}, \mathcal{P}$ and $\mathcal{C}$ are each delimited by regular ellipsoids as follows:

$$\mathcal{M} = \left\{ (x,y,z) \in \mathbb{R}^3 : \left(\frac{x^2}{a_x^2} + \frac{y^2}{a_y^2} + \frac{z^2}{a_z^2} \right) \leq r_{\mathcal{M}} \right\} \tag{4}$$

$$\mathcal{P} = \left\{ (x,y,z) \in \mathbb{R}^3 : \left(\frac{x^2}{a_x^2} + \frac{y^2}{a_y^2} + \frac{(z - r_{\mathcal{P}} + r_{\mathcal{M}})^2}{a_z^2} \right) \leq r_{\mathcal{P}} \right\} \setminus \mathcal{M} \tag{5}$$

$$\mathcal{C} = \left\{ (x,y,z) \in \mathbb{R}^3 : \left(\frac{x^2}{a_x^2} + \frac{y^2}{a_y^2} + \frac{(z - r_{\mathcal{C}} + r_{\mathcal{M}})^2}{a_z^2} \right) \leq r_{\mathcal{C}} \right\} \setminus \mathcal{P} \tag{6}$$

This basic structure is illustrated in Fig. 3. Note that cortex and medulla are not connected, which is not always the case [15].

3.3 Assumptions and Limitations

The model presented here is still extremely simplified. The standard random walk is not a realistic model of cell migration, as pointed out by Beltman et al. [18]: "abrupt directional changes are not possible because it takes time to displace the complicated internal structure that brings about motion". Indeed, histograms of T cell turning angles generated from intravital microscopy data show a significant deviation from a true random walk [19, 13]: smaller turning angles are favoured. Moreover, T cells move in rhythmic patterns where phases of high velocities alternate with pauses.

However, from statistics, we know that most processes that behave "roughly" like a random walk and have a finite mean square step size will spread out like normal diffusion. This follows from the central limit theorem [24]. Since we are focusing on the mesoscopic to macroscopic scale, approximating the motility of

T cells by a standard random walk should suffice as long as the T cell motility coefficient [11] is reproduced.

The absence of B cells is problematic for the analysis of compartmentalization. Effects like expulsion of T cells from the cortex are not taken into account. However, assuming a standard random walk, the tracks of individual cells are independent. Thus, adding B cells would not change the resulting dynamics.

Finally, entry and exit are modelled in a too simple manner. High endothelial venules are not explicitly represented, new lymphocytes just "appear" in the lymph node. We accept this for now since HEVs only make up about 1% of the paracortical area [25]. The exit process has not been modelled more explicitly since the amount of time T cells spend in the medulla is rather small [6]. All these simplifications have to be taken into account when interpreting our results.

4 Results

The default parameters used in our simulations are given in table 1 along with the corresponding literature references. However, some of the parameters could not be inferred from literature. The choice of the entry term $\boldsymbol{e}(t, v)$ depends on the distribution of high endothelial venules (HEVs) across the paracortex. Even though it is generally assumed that HEVs tend to lie close to the cortex, we are not aware of any reliable data on this. So we initially assume that the HEVs are uniformly distributed and set $\boldsymbol{e}(t, v) = 1/|\mathcal{P}|$. Values for $\boldsymbol{\sigma}$ and $\boldsymbol{l}$ will be derived in the next section.

4.1 Compartmentalization

In order to investigate the influence of the stickiness parameter $\boldsymbol{\sigma}$ on the concentrations of T cells in cortex and paracortex, we have calculated the equilibrium concentration $\bar{T}$ where for all $v \in V : \bar{T}(t+\Delta t, v) = \bar{T}(t, v)$. This can be done by combining 1 to 2 with the equilibrium condition into a system of linear equations with the unique solution $\bar{T}$. We have found that if $\boldsymbol{e}(t, v)$ is sufficiently small with respect to $\bar{T}(t, v)$ and the variance of $\bar{T}(t, v)$ is sufficiently small across $\mathcal{C}$, the paracortex/cortex ratio of T cell concentration is approximately

$$\frac{\sum_{v\in\mathcal{C}} \bar{T}(t, v)/v^+(v)}{\sum_{v\in\mathcal{P}} \bar{T}(t, v)/v^+(v)} \approx \frac{1}{|\mathcal{B}|} \sum_{v\in\mathcal{B}} \frac{|v^+(v)| - (1-\boldsymbol{\sigma})|c^+(v)|}{(1-\boldsymbol{\sigma})|v^+(v) \setminus c^+(v)|} \tag{7}$$

Note that 7 depends only on $\boldsymbol{\sigma}$ and, to a lesser extent, on the shape of $\mathcal{B}$. Generally, the structure of $\mathcal{LN}$ is not important. This makes sense biologically since compartmentalization is still observed in morphologically degenerate lymph nodes [26]. Based on the approximation, the paracortex/cortex concentration ratio of T cells of about 11 (estimation based on counting cells on 2D microtome sections) should be reproduced by setting $\boldsymbol{\sigma}$ to about 0.88. Using our default parameters, this is indeed the case (see Fig. 4). Based on this result, we estimated $\boldsymbol{l}$ by visually matching slices of $\bar{T}$ to 2D microtome sections from entire lymph

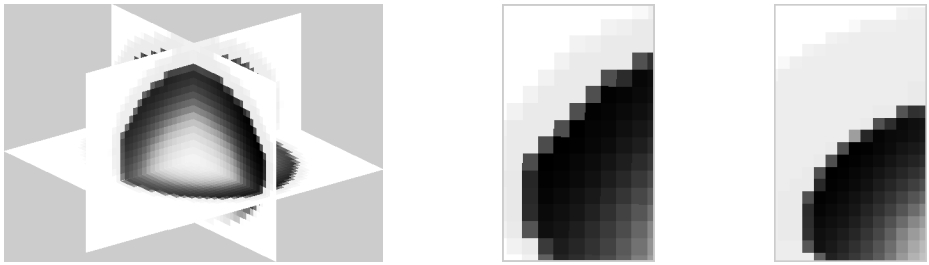

Fig. 4. Equilibrium concentration of 1 to 3 with default parameters (table 1). Left: 3D arrangement of xy,yz and xz slices. Center: Section similar to the one shown in Fig. 1, with sharply bounded compartments ($[\mathcal{P}]/[\mathcal{C}]$ ratio: 10.54; 7 gives 11.88). Right: 3-fold enlargement of the cortex ($r_{\mathcal{C}} = 0.6$mm) hardly influences the boundary ($[\mathcal{P}]/[\mathcal{C}]$ ratio: 10.62; 7 gives 11.98).

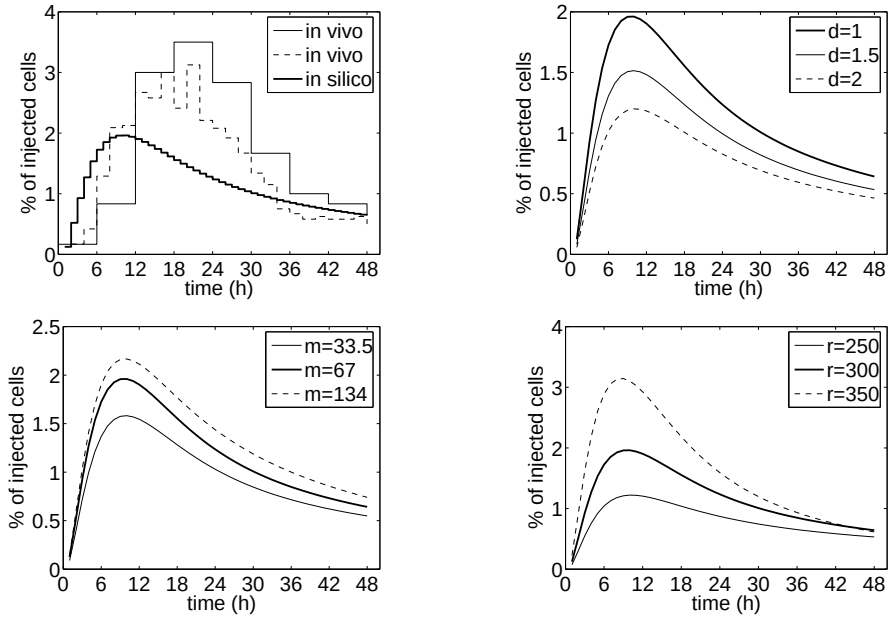

Fig. 5. Rates at which injected lymphocytes leave the lymph node plotted as a function of time. Top left: percentages of injected lymphocytes reappearing in thoracic duct (dashed: [27], collected in 2h-intervals; solid: [28], collected in 6h-intervals) plotted vs. the exit rate of our model with default parameters. Top right: The entire lymph node was scaled by d. Lymph node diameters between 1 and 2 mm are typical for mice, rats and humans; setting $d = 10$mm would reduce the peak to 0.2%. Bottom left: Modification of the T cell motility coefficient to 50% and 200% of its original value of $67\mu m^2$/min [11]. Bottom right: The kinetics are highly sensitive to modifications of the radius of the medulla (legend units are given in μm).

nodes ([15], own archives). $\boldsymbol{l} = 0.995$ generated both a sufficiently homogeneous concentration in the paracortex and a reasonable decrease of concentration in the medulla.

4.2 Recirculation Kinetics

Upon exit from lymph nodes, lymphocytes enter lymphatic vessels which drain into the thoracic duct. In a common experimental setup, labelled lymphocytes are injected into the blood. The reappearance of these lymphocytes in the thoracic duct is then measured as a function of time. The characteristics of these *recirculation kinetics* have been independently confirmed by many authors (see [20] for various sources) and are thus suitable for the validation of our model.

To be able to do this, we have included the process of lymphocyte recruitment in HEVs. Upon injection, the lymphocyte labelling index in the blood decreases exponentially. 50% of the initial value are reached after about 30 min [25, 27]. After 2 hours, 50% of lymphocytes have migrated through the wall of the HEV into the paracortex [6]. We combined these two processes by setting $\boldsymbol{e}(v,t) = \exp(-\ln(2)(t)/150(t+1))$ (since $\Delta t = 1\text{min}$).

Results are shown in Fig. 5: Our results are comparable to those obtained *in vivo*, but the mean T cell residence time is significantly lower. There are several possible reasons for this: (i) a fraction of the injected lymphocytes have long-lasting contacts with DCs and thus remain longer in the lymph node, which is not accounted for in our model; (ii) T cell migration might be non-uniform in time, e.g. the cells start slowly upon lymph node entry, accelerating their movement after some time when no matching antigen is found; (iii) T cells could be retained in the lymph node by chemokines; however, this is unlikely, since the S1P chemokine gradient which exists between blood and SLOs rather seems to guide T cells out of the lymph node [29]. Our estimation for now is that (ii) and (iii) are responsible for the difference in residence time, since T cell priming by dendritic cells has been shown to occur in three distinct phases with different motilities [13].

5 Conclusions and Future Work

We have created a simple mesoscopic-scale model of naive T cell entry, migration and exit in the lymph node. We have shown how a simple local mechanism may give rise to compartmentalization into cortex and paracortex. Explicit simulations of recirculation experiments have yielded results that are comparable to those found by experiments, but show a significantly lower T cell residence time. This indicates the existence of a mechanism which alters the T cell random walk over time.

The next steps will be to model the exit process more explicitly and to gradually incorporate B cells as more reliable results on their migratory patterns become available. But most importantly, a profound mathematical understanding of the proposed model has to be gained.

Symbol	*Space*	*Default*	*Meaning*	*Sources*
$r_{\mathcal{M}}$ $r_{\mathcal{C}}$ $r_{\mathcal{P}}$	$\mathbb{R}^+$	$300\mu m$ $450\mu m$ $500\mu m$	Base radii of medulla, cortex and paracortex	[10, 15, 25]
a_x a_y a_z	$[0,1]$ $[0,1]$ $[0,1]$	1 .8 .5	Relative sizes of ellipsoid main axes	[15, 26]
$\boldsymbol{\sigma}$	$[0,1]$	0.88	"Stickiness" of T cells to paracortex, related to T cell concentrations by 7	Cell counting on microtome sections
$\boldsymbol{e}(t,v)$	$[0,1]$	$1/\lvert\mathcal{P}\rvert$	Spatiotemporal distribution of T cell entry in paracortex	n/a
$\boldsymbol{m}$	$[0,1]$	$67\frac{\Delta s^2 \min}{\Delta t\, \mu m^2}$	T cell random walk motility	[11, 12, 7]
$\boldsymbol{l}$	$[0,1]$	0.005	Speed of exit process in medulla	Visual matching to microtome sections
Δs	$\mathbb{R}^+$	$20\mu m$	Spatial grid resolution, corresponds to mean length of FRC/FDC fibers	[10]
Δt	$\mathbb{R}^+$	1min.	Temporal resolution	

Table 1. Parameters of our model with their respective meanings, default values and sources. Microtome sections from our own archives were used for estimating σ and e.

References

1. Westermann, J., Pabst, R.: Distribution of Lymphocyte Subsets and Natural Killer Cells in the Human Body. Clin. Investig. **70** (1992) 539–544
2. Von Andrian, U. H., Mackay, C. R.: T-Cell Function and Migration. Two Sides of the Same Coin. N. Engl. J. Med. **343**(14) (2000) 1020–1032
3. Moser, B., Loetscher, P.: Lymphocyte Traffic Control by Chemokines. Nat. Immunol. **2**(2) (2001) 123–128
4. Reif, K., Ekland, E. H., Ohl, L., Nakano, H., Lipp, M., Förster, R., Cyster, J. G.: Balanced Responsiveness to Chemoattractants from Adjacent Zones Determines B-Cell Position. Nature **416** (2002) 94–99
5. Cyster, J.G.. Ansel, K.M., Reif, K., Ekland, E.H., Hyman, P., Tang, H.L., Luther, S.A., Ngo, V.N.: Follicular Stromal Cells and Lymphocyte Homing to Follicles. Immunol. Rev. **176** (2000) 181–193
6. Westermann, J., Engelhardt, B., Hoffmann, J.: Migration of T Cells In Vivo: Molecular Mechanisms and Clinical Implications. Ann. Intern. Med. **135** (2001) 279–295
7. Wei, S. H., Parker, I., Miller, M. J., Cahalan, M.D.: A Stochastic View of Lymphocyte Motility and Trafficking Within the Lymph Node. Immunol. Rev. **195** (2003) 136–159
8. Cenk, S., Mempel, T. R., Mazo, I. B., Von Andrian, U. H.: Intravital Microscopy: Visualizing Immunity in Context. Immunity **21** (2004) 315–329
9. Halin, C., Mora, J. R., Sumen, C., Von Andrian, U. H.: In Vivo Imaging of Lymphocyte Trafficking. Annu. Rev. Cell Dev. Biol. **21** (2005) 581–603

10. Bajénoff, M., Egen, J. G., Koo, L. Y., Laugier, J. P., Brau, F., Glaichenhaus, N., Germain, R. N.: Stromal Cells Networks Regulate Entry, Migration, and Territoriality in Lymph Nodes. Immunity **25** (2006) 1–13
11. Miller, M. J., Wei, S. H., Parker, I., Cahalan, M.D.: Two-Photon Imaging of Lymphocyte Motility and Antigen Response in Intact Lymph Node. Science **296** (2002) 1869–1873
12. Miller, M. J., Wei, S. H., Cahalan, M.D., Parker, I.: Autonomous T Cell Trafficking Examined In Vivo with Intravital Two-Photon Microscopy. PNAS **100** (2003) 2604–2609
13. Mempel, T., Henrickson, S. E., Von Andrian, U. H.: T-Cell Priming by Dendritic Cells in Lymph Nodes Occurs in Three Distinct Phases. Nature **427** (2004) 154–159
14. Okada, T., Miller, M.J., Parker, I., and Matthew F. Krummel, M.F., Neighbors, M., Hartley, S., O'Garra, A., Cahalan, M.D., Cyster, J.G.: Antigen-Engaged B Cells Undergo Chemotaxis toward the T Zone and Form Motile Conjugates with Helper T Cells. PLoS Biology **3**(6) (2005) 1047–1061
15. Ma, B., Jablonska, J., Lindenmaier, W., Dittmar, K.: Immunohistochemical Study of the Reticular and Vascular Network of Mouse Lymph Node Using Vibratome Sections. Acta Histochem. **109** (2007) 15–28
16. Seiden, P. E., Celada, F.: A Model for Simulating Cognate Recognition and Response in the Immune System. J. Theor. Biology. **158**(3) (1992) 329–357
17. Efroni, S., Harel, D., Cohen, I.R.: Toward Rigorous Comprehension of Biological Complexity: Modeling, Execution, and Visualization of Thymic T-Cell Maturation. Gen. Res. **13** (2003) 2485–2497
18. Beltman, J. B., Marée, A., Lynch, N. L., Miller, M.J., De Boer, R. J.: Lymph Node Topology Dictates T Cell Migration Behavior. J. Exp. Med. **204**(4) (2007) 771-780
19. Beltman, J. B., Marée, A., De Boer, R. J.: Spatial Modelling of Brief and Long Interactions between T Cells and Dendritic Cells. Imm. Cell Biol., in press
20. Stekel, D. J.: The Simulation of Density-Dependent Effects in the Recirculation of T Lymphocytes. Scand. J. Immunol. **47** (1998) 426–439
21. Stekel, D. J., Parker, C. E., Nowak, M. A.: A model of Lymphocyte Recirculation. Immunol. Today **18** (1997) 216–221
22. Beauchemin, C., Forrest, S., Koster, F.T.: Modeling Influenza Viral Dynamics in Tissue. In Bersini, C., Carneiro, J. (Eds.): ICARIS 2006, LNCS 4163, Springer (2006) 23–36
23. Murray, J.: Mathematical Biology. Springer, 1998.
24. Kallenberg, O.: Foundations of Modern Probability. Springer, 2002.
25. Blaschke, V., Micheel, B., Pabst, R., Westermann, J.: Lymphocyte Traffic Through Lymph Nodes and Peyer's Patches of the Rat: B- and T-Cell-Specific Migration Patterns Within the Tissue, and Their Dependence on Splenic Tissue. Cell Tissue Res. **282** (1995) 377–386
26. Uematsu, T., Sano, M., Homma, K.: In Vitro High-Resolution Helical CT of Small Axillary Lymph Nodes in Patients with Breast Cancer: Correlation of CT and Histology. Am. J. Roentgenol. **176** (2001) 1069–1074.
27. Westermann, J., Puskas, Z., Pabst, R.: Blood Transit and Recirculation Kinetics of Lymphocyte Subsets in Normal Rats. Scand. J. Immunol. **28** (1988) 203–210
28. Migration of So-Called Naive and Memory T Lymphocytes from Blood to Lymph in the Rat. J. Immunol. **152** (1994) 1744–1750
29. Schwab, S., Pereira, J., Matloubian, M., Xu, Y., Huang, Y., Cyster, J.: Lymphocyte Sequestration Through S1P Lyase Inhibition and Disruption of S1P Gradients. Science **309** (2005), 1735–1739